

## SUPPLEMENTARY MATERIAL

### In-situ atomic-resolution study of transformations in double polymorph $\gamma/\beta$ -Ga<sub>2</sub>O<sub>3</sub> structures

*J. García-Fernández\**, *S. B. Kjeldby*, *L. J. Zeng*, *A. Azarov*, *A. Pokle*, *P. D. Nguyen*, *E. Olsson*, *L. Vines*,  
*A. Kuznetsov\**, *Ø. Prytz\**

#### I. Displacement per atom calculations and irradiation parameters

The implantation parameters for the Au and Si ions were chosen in such a way to produce nearly the same distribution and number of primary defects as can be seen from Fig. S1 and Table SI summarizing the implantation parameters. As seen from Fig. S1 that despite the displacement per atom (DPA) depth profile produced by Si ions is broader and has a lower maximum as compared to that of Au ions, the profiles of these ions are comparable.

Note that the DPA vs depth profiles were calculated using conventional methodology [Ref. S1] based on SRIM code [Ref. S2] simulations. Specifically, the SRIM vacancy generation profiles for a given fluence were normalized to an atomic density of  $\beta$ -Ga<sub>2</sub>O<sub>3</sub> ( $n_{at} = 9.45 \times 10^{22}$  at/cm<sup>3</sup>). The SRIM simulations were performed with 28 eV and 14 eV as the displacement energies for Ga and O atoms, respectively [Ref. S3].

Ion	Energy (keV)	Fluence			$R_{pd}$ (nm)	$R_p$ (nm)	Max conc. (at.%)
		(ions/cm <sup>2</sup> )	1 dpa (ions/cm <sup>2</sup> )	(max dpa)			
<sup>28</sup> Si <sup>+</sup>	300	$2 \times 10^{16}$	$6.5 \times 10^{14}$	31	200	245	1
<sup>197</sup> Au <sup>+</sup>	1200	$3 \times 10^{15}$	$7.5 \times 10^{13}$	40	115	160	0.3

**Table SI.** Implant parameters used in the present study, where the ion fluences are shown also for the 1 DPA as well as maximum values of DPA are indicated for both ions. The  $R_{pd}$  and  $R_p$  indicate the depth where the defect generation profile is maximal and the projected range of the implanted ions, respectively.

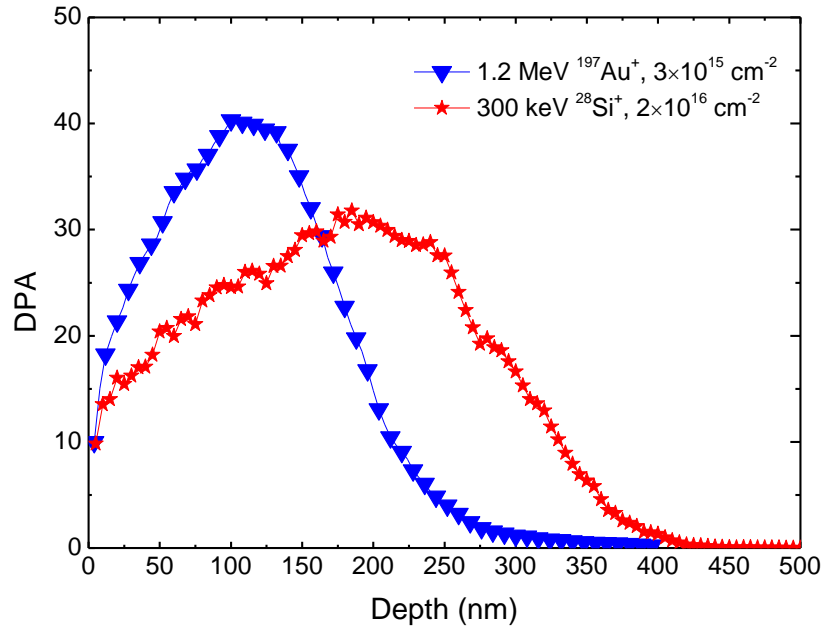


**Fig. S1.** DPA vs depth profiles in  $\beta$ -Ga<sub>2</sub>O<sub>3</sub> for Si and Au implants as indicated in the legend.

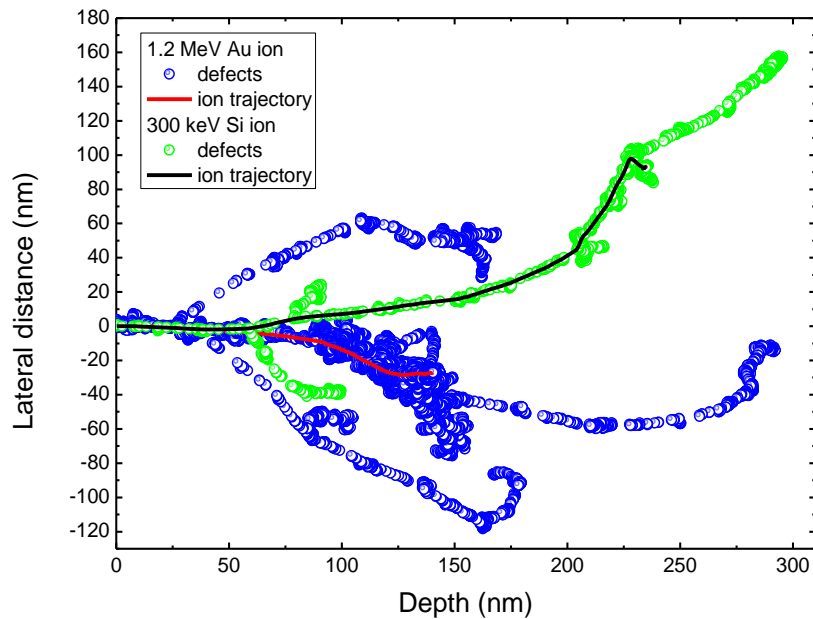


**Fig. S2.** Projections of individual collision cascades produced by 1.2 MeV Au and 300 keV Si ions in  $\beta$ -Ga<sub>2</sub>O<sub>3</sub> simulated using the SRIM code [Ref. S2]. The lines correspond to the ion trajectories while the circles correspond to the point defects.

However, it should be mentioned that the collision cascade shape as well as number of primary defects generated by one individual ion are different for Au and Si due to large difference in atomic masses of these ions. Indeed, Fig. S2 illustrates the difference in the volumetric defect distribution in the  $\beta$ -Ga<sub>2</sub>O<sub>3</sub> samples for the single Au and Si implants. It is clearly seen that in contrast to Si ions, heavy Au ions generate dense collision cascade involving many large subcascades. Such difference in volumetric defect distribution and, therefore, in the density of collision cascades can result in the disorder enhancement attributed to the nonlinear defect interaction within collision cascade volume [Ref. S4].

## II. STEM analysis of the Au as-implanted and low-temperature annealed sample

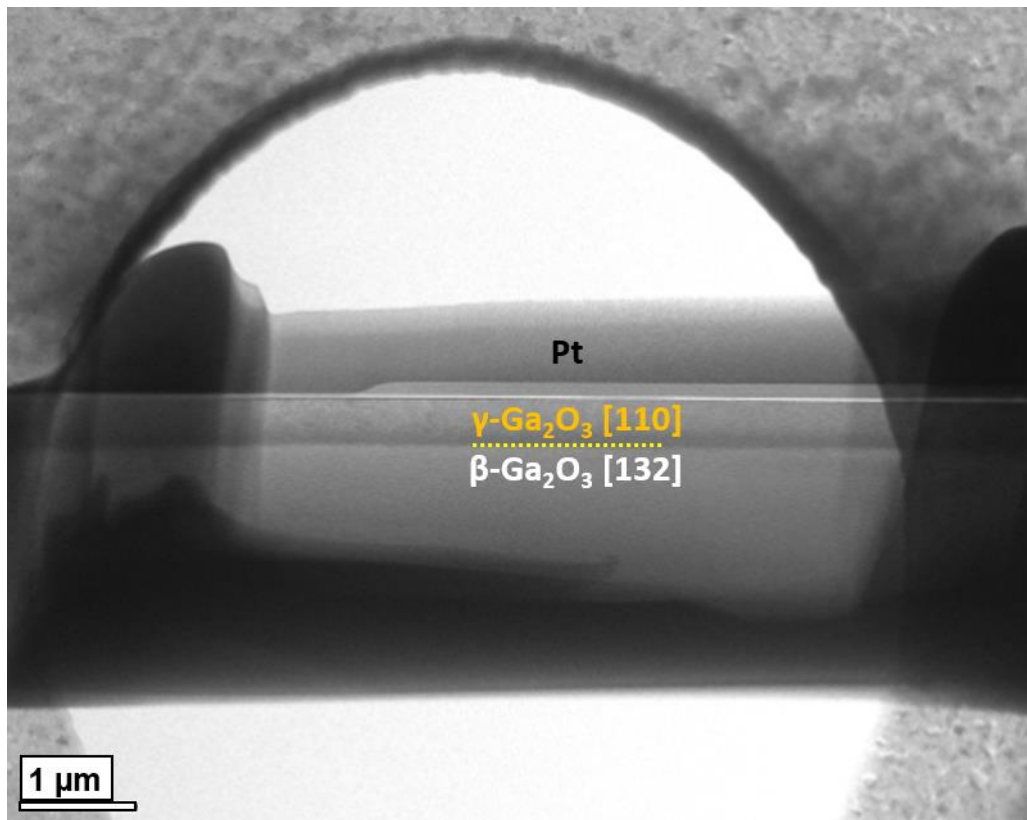


**Fig. S3.** Low magnification BF STEM image of the Au-implanted sample as fabricated in the heating E-chip showing the starting state of the double  $\gamma/\beta$ -Ga<sub>2</sub>O<sub>3</sub> polymorph structure.

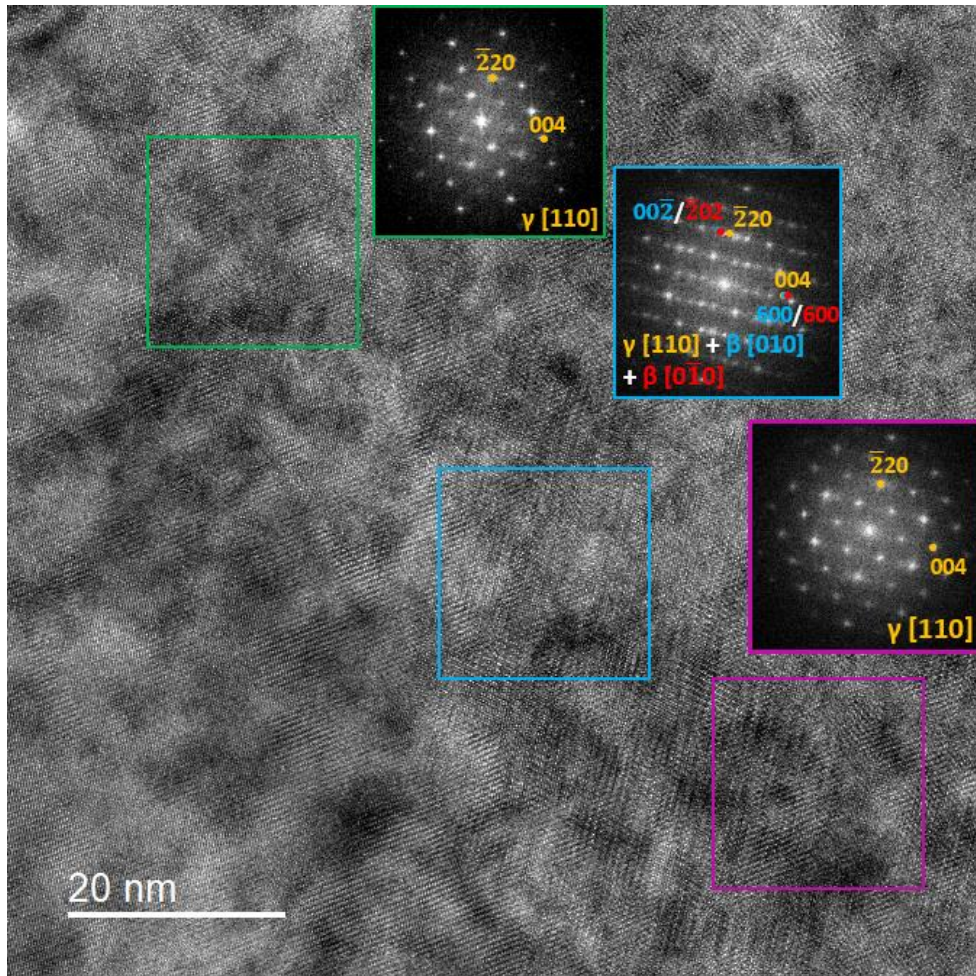


**Fig. S4.** HRTEM and corresponding FFT of different areas of the Au-implanted sample after annealing at 300°C. The formation of  $\beta$ -Ga<sub>2</sub>O<sub>3</sub> domains can be detected in the sample.

III. Oxygen-K edge analysis by EELS on the Si as-implanted and annealed sample

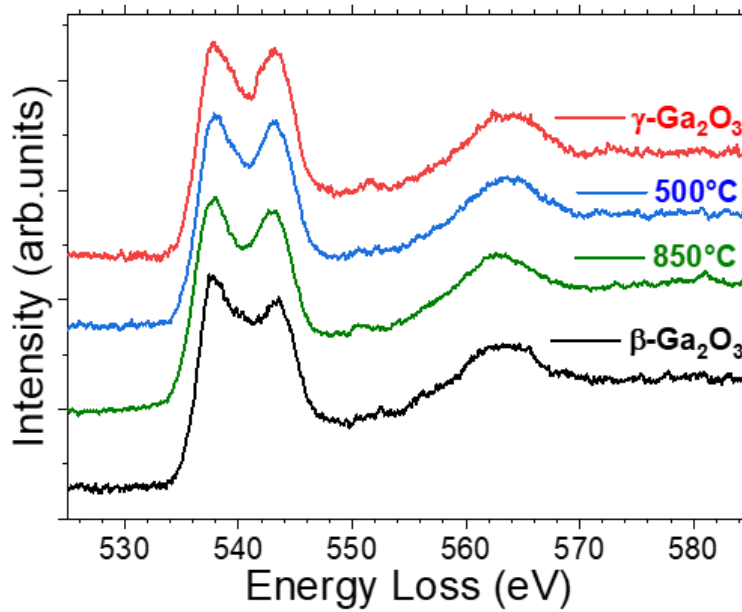


**Fig. S5.** EELS spectra of the oxygen-K edge, acquired from the as-implanted  $\gamma\text{-Ga}_2\text{O}_3$  (red), and after annealing at 500°C (blue) and 850°C (green), together with bulk  $\beta\text{-Ga}_2\text{O}_3$  (black). The obtained ratio between the two maxima centered at 537 and 543 eV is 1.02, 1.05, 1.14, and 1.21 for  $\gamma\text{-Ga}_2\text{O}_3$ , 500°C, 850°C, and  $\beta\text{-Ga}_2\text{O}_3$  samples, respectively, confirming the gradual transformation from  $\gamma$ - to  $\beta\text{-Ga}_2\text{O}_3$ .

Ref. S1. A. I. Titov, A. Yu. Azarov, L. M. Nikulina, and S. O. Kucheyev, "Damage buildup and the molecular effect in Si bombarded with PFn cluster ions", *Nucl. Instrum. Methods Phys. Res. B* **256**, 207 (2007).

Ref. S2. J. F. Ziegler, M. D. Ziegler, and J. P. Biersack, "SRIM—the stopping and range of ions in matter (2010)", *Nucl. Instrum. Methods Phys. Res. B* **268**, 1818 (2010).

Ref. S3. B. R. Tuttle, N. J. Karom, A. O'Hara, R. D. Schrimpf, and S. T. Pantelides, "Atomic-displacement threshold energies and defect generation in irradiated  $\beta\text{-Ga}_2\text{O}_3$ : A first-principles investigation", *J. Appl. Phys.* **133**, 015703 (2023).

Ref. S4. A. Azarov, V. Venkatachalapathy, P. Karaseov, A. Titov, K. Karabeshkin, A. Struchkov, and A. Kuznetsov, "Interplay of the disorder and strain in gallium oxide" *Scientific Reports* **12**, 15366 (2022).